



Research article

Seasonal variation in characteristics of wear microparticles of high density ($> 1.8 \text{ g cm}^{-3}$) produced on road

Uiyeong Jung, Sung-Seen Choi*

Department of Chemistry, Sejong University, 209 Neungdong-ro, Gwangjin-gu, Seoul, 05006, Republic of Korea

ARTICLE INFO

Keywords:

Wear microparticle
Road dust
Asphalt pavement road
High density
Bitumen

ABSTRACT

Wear microparticles are produced on roads by traffic, and they can be transferred to rivers and seas settling as sediments. The sedimentation rate increases with increasing particle density and size. In this study, the types and amounts of high-density wear microparticles (HDWPs, $>1.8 \text{ g cm}^{-3}$) in road dust were investigated. The HDWPs ranging from 106 to 1000 μm were classified into eight categories depending on the color, shape, and physical property: mineral particles (MPs), asphalt pavement wear particles (APWPs), glass particles (GPs), glass beads (GBs), tire-road wear particles (TRWPs), plant-related particles (PRPs), road paint wear particles (RPWPs), and plastic particles (PPs). The HDWPs in road dust were the most abundant in winter (94.0–95.6 wt%), while being the lowest in spring (82.7–90.7 wt%). MPs accounted for over 50 wt% of the HDWPs; however, TRWPs were not found in HDWPs larger than 200 μm . The HDWPs produced by the abrasion of roads, including asphalt pavements and marking paint, exceeded 90 wt%. The non-crosslinked organic components in the HDWPs were removed by chloroform treatment. The chloroform-soluble components in the HDWPs were much more present in winter than in other seasons. Swelling TRWPs with chloroform released mineral particles on the surface.

1. Introduction

Globally, 90 % of paved roads use asphalt as paving material [1–3]. Generally, asphalt pavement consists of over 95 wt% of aggregates, binders, and modifiers [4–7]. Because road markings must be visible to drivers even when driving at night, glass beads are mixed with road marking paint for retroreflection [8,9]. While driving, abrasion of roads and tires occurs due to the friction between the tire tread of the vehicle and the pavement surface to produce various wear particles, such as mineral particles (MPs), asphalt pavement wear particles (APWPs), glass particles (GPs), glass beads (GBs), tire-road wear particles (TRWPs), plant-related particles (PRPs), road paint wear particles (RPWPs), and plastic particles (PPs) [10–14].

These wear particles can exist in microscopic sizes, and can cause air, terrestrial, and aquatic environmental pollution by floating in the air or through water flows, such as rainwater or runoff [10,15–18]. Further, they exhibit different density ranges [11–13]. MPs, whose densities are $>1.8 \text{ g cm}^{-3}$, are the most abundant particles in road dust, whereas PRPs and PPs are found in a wide range of densities $>1.1 \text{ g cm}^{-3}$. TRWPs, APWPs, and RPWPs have densities of greater than 1.2, 1.4, and 1.6 g cm^{-3} , respectively, while GPs and GBs have densities $>1.6 \text{ g cm}^{-3}$. Road dust can be transferred to rivers and seas, where they settle as sediments, and the sedimentation velocity of a particle is proportional not only to its density but also to its size [19–22].

Bitumen used for asphalt pavement as a binder contains polycyclic aromatic hydrocarbons (PAHs) which in turn can be released

* Corresponding author.

E-mail address: sschoi@sejong.ac.kr (S.-S. Choi).



Fig. 1. Map of the sampling site.

from bitumen to the environment [23–25]. Since APWPs contain bitumen component, PAHs can be released from APWPs to the environment. Tire wear particles (TWPs) contain potentially harmful chemicals such as benzothiazole (BTH), benzotriazole (BTR), N-(1,3-dimethylbutyl)-N'-phenyl-1,4-phenylenediamine (6PPD), diphenylguanidine (DPG), and their derivatives, which can also be released to the environment [26–28]. Hence, the accumulation of APWPs and TRWPs in river and sea as sediment may result in the continuous release of toxic chemicals to the aquatic ecosystem.

Wear particles with high density can easily sink in water to form sediment, since their sedimentation rates are greater than those with lower density. Thus, researches on the types and amounts of wear particles with high density in road dust help understand the sedimentation of road dust in aquatic system. For this reason, in this study, the types and amounts of wear particles with high density in road dust were investigated. Road dust was collected at a bus stop during four seasons, and was separated by size to select wear microparticles of 106–1000 μm . The road dust samples with high density ($>1.8 \text{ g cm}^{-3}$) were prepared by density separation using an NaI aqueous solution. The high density wear microparticles (HDWPs) were classified into eight categories (MP, APWP, GP, GB, TRWP, PRP, RPWP, and PP) using a microscope, and their properties were characterized. Uncrosslinked organic components in the HDWPs, such as binders and modifiers, were examined by treating them with chloroform.

2. Materials and methods

2.1. Collection and size separation of road dust

Road dust was collected at a bus stop on a six-lane road nearby Sejong University, Republic of Korea ($37^{\circ}32'59.1''\text{N}$ $127^{\circ}04'32.3''\text{E}$, Fig. 1) in the winter (January 14th, 2021), spring (April 14th, 2021), summer (July 14th, 2021), and fall (October 20th, 2021) seasons. Road dust accumulated between the kerb and road at the bus stop was gathered by sweeping the road surface using a brush and broom, and then stored in a glass vial. The road dust samples were separated by size using a sieve shaker (Octagon 200, Endecotts Co., UK). Standard sieves of 1000, 500, 212, and 106 μm were used. Size separation was performed with the interval mode for 20 min. The road dust samples with size ranges of 106–212, 212–500, and 500–1000 μm were characterized.

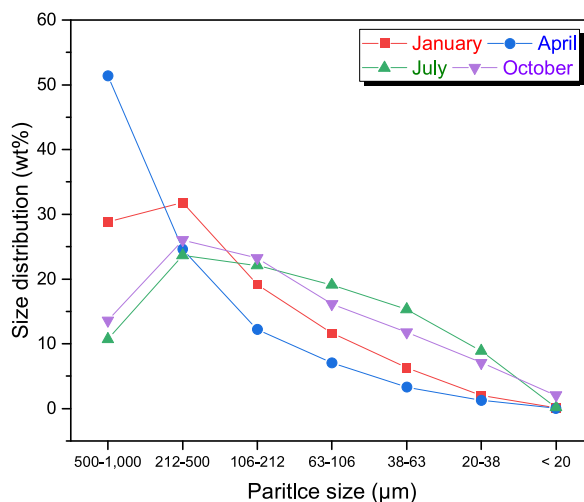


Fig. 2. Particle size distributions of the road dust samples. The squares, circles, up-triangles, and down-triangles stand for the road dust samples collected in the winter, spring, summer, and fall seasons, respectively.

2.2. Preparation of road dust sample with density higher than 1.8 g cm^{-3}

Road dust samples with density over 1.8 g cm^{-3} were prepared by density separation to obtain the wear microparticles of high density ($>1.8 \text{ g cm}^{-3}$) produced on road. An aqueous solution with density of 1.8 g cm^{-3} was prepared with sodium iodide (NaI, purity: 99.0 %, Ducksan Co., Republic of Korea) and distilled water. The solution density was checked using its weight and volume. The NaI solution of 50 mL was poured in a beaker with a diameter of 70 mm and a height of 40 mm, the road dust sample was put into the solution, and then left for 3 h. The particles with density $>1.8 \text{ g cm}^{-3}$ were sunk, whereas the other light particles remained floating. After removing the particles floated on the aqueous solution, the high density particles were filtered using a filter paper of 70 mm diameter (Whatman, England), washed with distilled water three times and with ethanol, and then dried at room temperature.

2.3. Classification of types of the wear microparticles

Morphology of the particles in the high density road dust was examined using a digital microscope of DM4M (Leica Microsystems, Germany). The high density wear microparticles (HDWPs) were classified into the 8 categories of MP, APWP, GP, GB, TRWP, PRP, RPWP, and PP, depending on the color, shape, and physical property. MPs have a rigid and angular shape, while APWPs are inelastic and break when pressed. GPs are transparent and angular shape, while GBs are spherical. TRWPs are black and elastic particles with elongated or round shapes. PRPs can be crushed into smaller pieces when pressed. RPWPs are white or yellow color and crumble when pressed, while PPs are thin and relatively hard.

2.4. X-ray fluorescence (XRF) analysis

The elemental composition of the sample was analyzed using a handheld XRF instrument, S1 Titan 800 (Bruker Co., USA). An Rh target tube was installed, the spot size was 8 mm, and the GeoExploration method was used. X-rays were examined for 40 s in three phases: 15 kV (No filter), 30 kV (Ti:25/Al:300 filter), and 50 kV (Cu:75/Ti:25/Al:200 filter). The characteristic X-rays emitted from the samples were detected by a 20 mm^2 silicon drift detector (SDD). During the analysis, the instrument was used in a fixed state using a desktop stand. The element range from Mg to U was analyzed for a total of 120 s. Besides metal components in APWPs, sulfur (S) and zinc (Zn) components in TRWPs were also analyzed.

2.5. Chloroform treatment

In order to remove uncrosslinked organic components such as bitumen and uncrosslinked rubber chains in the sample, the HDWPs were soaked in chloroform (Samchun Chemical Co., Republic of Korea). The uncrosslinked organic components-removed sample was washed with chloroform and dried. The sample weights were 30, 20, and 10 mg for the wear particles of 500–1000, 212–500, and 106–212 μm , respectively. The sample weights before and after the chloroform treatment were measured, and the weight difference was used as the amount of the uncrosslinked organic components in the sample.

Table 1
Temperature ranges on the road dust sampling date and 7 days before the sampling.

Season	Date	Temperature range
Winter	January 07–14, 2021	−18.6 °C – 8.3 °C
Spring	April 07–14, 2021	3.1 °C–20.4 °C
Summer	July 07–14, 2021	23.1 °C–33.5 °C
Fall	October 13–20, 2021	4.2 °C–25.2 °C

Table 2
Ratios of the wear particles with high density ($>1.8 \text{ g cm}^{-3}$) in the road dust samples (wt%).

Season	Wear particle size (μm)		
	106–212	212–500	500–1000
Winter	94.0	95.6	95.4
Spring	85.7	90.7	82.7
Summer	89.5	91.5	89.6
Fall	86.6	91.9	88.0

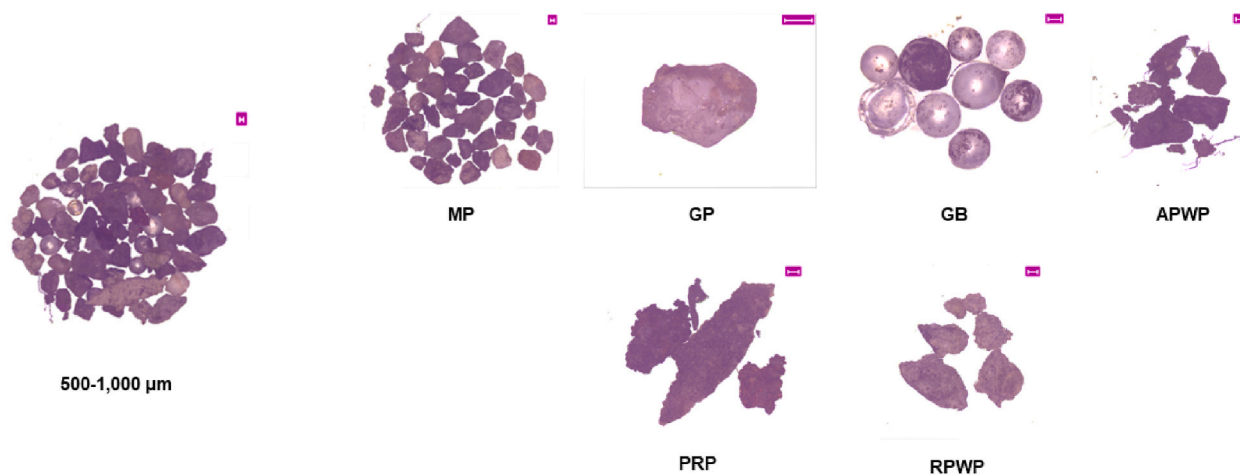


Fig. 3. Magnified images ($\times 50$) of the high density wear particles of 500–1000 μm . The road dust sample was collected in the winter season and the sample weight in the image was 30 mg. The scale bar is 200 μm .

3. Results and discussion

3.1. Particle size distributions of the road dust samples

The particle size distributions of the road dust samples showed two opposite patterns (Fig. 2). The particle size distributions of the road dust samples collected in winter (January) and spring (April) decreased as the particle size decreased; however, those collected in summer (July) and fall (October) tended to increase with an increase in particle size. This significant difference may be due to the differences in road temperatures. Temperatures were lower in winter and spring than in summer and fall (Table 1). The particle size distribution of the road dust samples collected in spring displayed a similar pattern to that of the road dust samples collected in winter, although spring was warmer than winter. This may be because the fatigue that accumulated on the road during the cold season did not completely recover until spring. Similarly, the road conditions formed during the hot season may be maintained during early fall. The difference in the particle size distributions indicated that larger particles were generated from the road due to traffic as the temperature decreased. Road dust is composed of various components including wear particles from tires and pavements and external sources such as soil [10–14]. Thus, the particle size distribution of road dust is influenced by various factors like traffic conditions, road pavement conditions, and contribution of the external source [10,36–38].

Wear microparticles with high density ($>1.8 \text{ g cm}^{-3}$) (HDWPs) in road dust samples of size 106–212, 212–500, and 500–1000 μm were selected by the density separation. The ratios of HDWPs in the road dust samples are summarized in Table 2. The ratios of HDWPs in the road dust samples were higher than 80 wt% (82.7–95.6 wt%). The HDWP ratios were the highest and lowest in the winter (94.0–95.6 wt%) and spring (82.7–90.7 wt%), respectively. The average HDWP contents in road dust of 106–1000 μm were calculated by considering the size distribution and each HDWP ratio, and were 95.1 wt%, 85.3 wt%, 90.4 wt%, and 89.1 wt% for the winter,

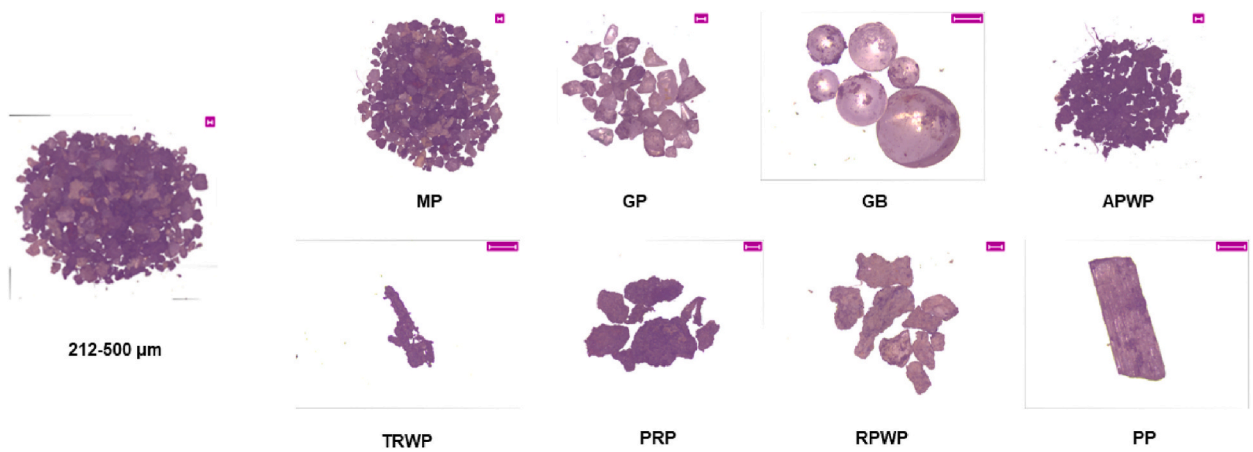


Fig. 4. Magnified images ($\times 50$) of the high density wear particles of 212–500 μm . The road dust sample was collected in the winter season and the sample weight in the image was 20 mg. The scale bar is 200 μm .

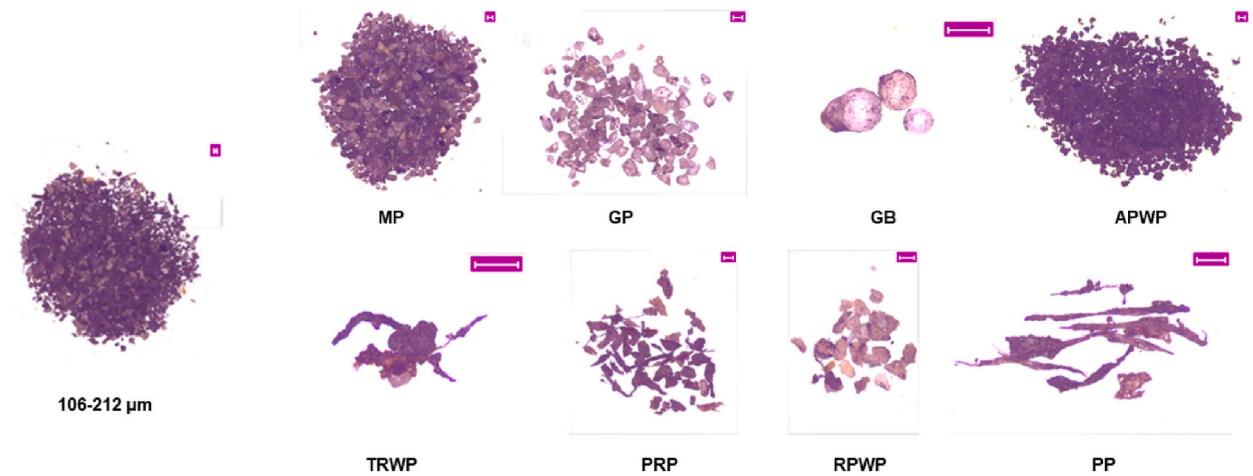


Fig. 5. Magnified images ($\times 50$) of the high density wear particles of 106–212 μm . The road dust sample was collected in the winter season and the sample weight in the image was 10 mg. The scale bar is 200 μm .

Table 3

Distributions of the various wear particles with high density ($>1.8 \text{ g cm}^{-3}$) in the road dust sample collected during winter (wt%).^a

Wear particle	Wear particle size (μm)		
	106–212	212–500	500–1000
MP	56.3	77.6	75.1
APWP	20.0	9.4	6.7
GB	0.4	1.7	10.4
GP	20.7	7.3	0.9
RPWP	0.9	1.7	3.6
TRWP	0.1	trace	–
PRP	1.5	1.2	3.3
PP	0.1	1.1	–

^a MP (mineral particle), GP (glass particle), APWP (asphalt pavement wear particle), GB (glass bead), TRWP (tire-road wear particle), PRP (plant-related particle), RPWP (road paint wear particle), PP (plastic particle).

spring, summer, and fall seasons, respectively. The order of average HDWP content according to the season was winter $>$ summer $>$ fall $>$ spring. The differences in HDWP ratios during summer and fall were not significant. The HDWP ratios in the road dust samples of size 212–500 μm were greater than those of size 106–212 and 500–1000 μm .

Table 4
Distributions of principal elements in the wear particles with high density ($>1.8 \text{ g cm}^{-3}$) in the road dust samples (%).

Particle size (μm)	Element				
	Al_2O_3	SiO_2	S	Fe	Zn
Winter					
106–212	4.81	27.53	0.24	1.45	0.11
212–500	4.43	32.20	0.20	1.29	0.03
500–1000	3.67	34.85	0.20	2.32	0.02
Spring					
106–212	3.38	19.58	0.08	1.26	0.05
212–500	4.86	38.24	0.11	1.18	0.02
500–1000	3.98	24.99	0.07	0.90	0.03
Summer					
106–212	4.39	27.87	0.06	1.08	0.04
212–500	4.63	39.66	0.08	1.16	0.02
500–1000	4.28	34.46	0.21	1.02	0.02
Fall					
106–212	0.67	3.84	0.07	0.03	0.09
212–500	0.76	4.80	0.06	0.11	0.06
500–1000	0.93	5.23	0.08	0.14	0.03

3.2. Variety of wear microparticles in road dust

HDWPs within the 106–1000 μm size range were meticulously classified under a microscope, as depicted in Figs. 3–5 for the samples with the size ranges of 500–1000, 212–500, and 106–212 μm , respectively. The types of HDWPs were classified into eight categories: MP, GB, GP, APWP, TRWP, PRP, RPWP, and PP. The sources of MPs include abraded aggregates used for asphalt pavements and the inflow of soil from the outside. GPs used as mineral fillers for asphalt pavements exhibit an angular morphology, whereas GBs present a spherical form, and are used in road marking paint to enhance retroreflection [29]. Both APWPs and TRWPs are black; however, TRWPs are elastic particles with elongated or round shapes, whereas APWPs are inelastic and break easily under pressure [11–13]. PRPs originate from plants surrounding the sampling site, and RPWPs result from the degradation of road marking paint due to traffic. Wear microparticles generated by the abrasion of asphalt pavements include APWPs and large portions of MPs, RPWPs, GPs, and GBs.

Among the eight types of wear particles, no TRWPs and PPs were present in the road dust sample of size 500–1000 μm (Fig. 3). The distributions of HDWP types in road dust samples collected during winter are summarized in Table 3. MPs were the most abundant particle type because they originate from the abrasion of road pavement and the inflow of soil components from the outside. The distribution of MPs increased with increasing particle size. The distribution of APWPs notably decreased from 20.0 wt% to 6.7 wt% when the particle size increased from 106–212 μm to 500–1000 μm . The distribution of GBs significantly increased from 0.4 wt% to 10.4 wt% as the particle size increased from 106–212 μm to 500–1000 μm , whereas that of GPs largely decreased from 20.7 wt% to 0.9 wt%. These different results can be explained by the size of the GBs used for retroreflection and the source of the GPs. The GBs used for road marking paint have a relatively wide size range, from 20 mesh (850 μm) to 100 mesh (150 μm), and GPs with relatively large particle sizes are mainly used. Because wear particles of GPs used as asphalt pavement fillers are generated by abrasion of the pavement road, their size becomes smaller due to friction between the road surface and the tire tread. The distribution of RPWPs increased from 0.9 wt% to 3.6 wt% when the particle size increased from 106–212 μm to 500–1000 μm .

The order of particle type distribution in the 106–1000 μm HDWP was MP (69.67 wt%) > APWP (12.03 wt%) > GP (9.63 wt%) > GB (4.17 wt%) > RPWP (2.07 wt%) > PRP (2.00 wt%) > PP (0.40 wt%) > TRWP (0.03 wt%). Since GB is used in road marking paint, the content of wear particles of road marking paint (GB + RPWP) will be over 6 wt%. Wear microparticles generated from road abrasion, including asphalt pavement and road marking paint, include APWPs, MPs, GBs, GPs, and RPWPs. Without considering the outside source of MPs, wear microparticles sourced from the road amounted to 98.3, 97.7, and 96.7 wt% in HDWPs of size 106–212, 212–500, 500–1000 μm , respectively. It can be concluded that approximately 95 wt% of the HDWPs originated from road abrasion, including asphalt pavement and road marking paint. TRWPs with a high density were not observed in the road dust sample of size 500–1000 μm , were rarely detected in the road dust sample of size 212–500 μm , and were found in less than 0.1 wt% for the road dust sample of size 106–212 μm . TRWPs produced on real roads are usually smaller than 200 μm , irrespective of the density [11,26].

3.3. XRF analysis results

The XRF analysis results for the principal elements of the HDWP sample are summarized in Table 4. There were no detectable toxic heavy metals such as Pb, Cd, and Hg in the samples. Their detection limits in XRF analysis are 7, 5, and 10 ppm, respectively. Al_2O_3 and SiO_2 were the main components of MPs, GBs, and GPs. Sulfur (S) and zinc (Zn) can be obtained from tire tread compounds containing zinc oxide (ZnO), sulfur, and sulfur cure accelerators [30–32]. Moreover, there are various sulfur sources such as bitumen, exhaust gas, and aggregates as well as TWPs [33,34]. The iron (Fe) component may have been partly derived from brake wear particles [35]. Other Fe sources can be aggregates of pavement and soil come from the outside.

Zn was detected in trace amounts, but it could not wholly originate from TRWPs because TRWPs of size 500–1000 μm were not

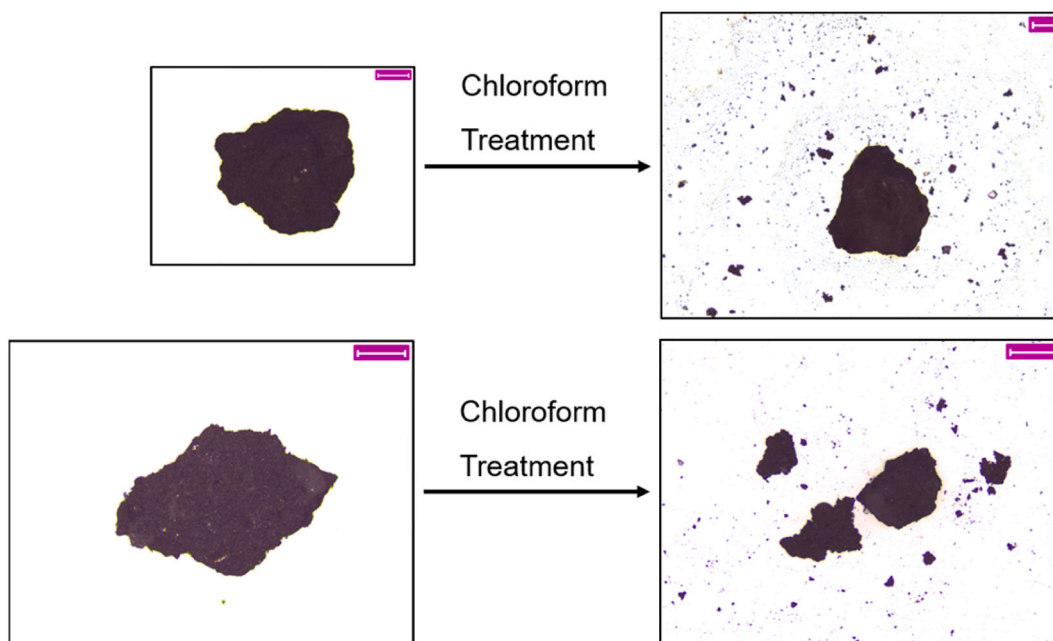


Fig. 6. Magnified images ($\times 50$) of the asphalt pavement wear particles (APWPs) before and after the chloroform treatment. The scale bar is $200 \mu\text{m}$.

observed. Because the Zn content in the samples of $500\text{--}1000 \mu\text{m}$ was at least 0.02% , the minimum content of Zn from other sources, and not abrasion of the tire tread, should be 0.02% . The Zn contents in the samples of size $106\text{--}212 \mu\text{m}$ were much higher than those in the samples of size $212\text{--}500$ and $500\text{--}1000 \mu\text{m}$, which implies that some TRWPs are present in the samples of size $106\text{--}212 \mu\text{m}$. Variations of the sulfur content with the particle size did not show any trends, which means that the sulfur sources in road dust vary, as discussed above. The Fe contents did not show a specific trend depending on the particle size, however, the Fe contents in the sample collected in the winter season were greater than those in the samples collected during other seasons, which was related to high abrasion of the brake in the cold season. The contents of Al_2O_3 and SiO_2 were smaller in the fall than in other seasons. This may be due to less inflow of soil components from the outside.

3.4. Amounts of uncrosslinked organic components in HDWPs

Chloroform is a good solvent for dissolving uncrosslinked organic components in road dust such as bitumen, uncrosslinked rubber components, and others. Styrene-butadiene-styrene block copolymer (SBS, uncrosslinked rubber) can be used as a modifier for asphalt pavement [39]. Following the chloroform treatment, the APWPs were divided into many particles as shown in Fig. 6. This means that many small particles combined with binders, such as bitumen and uncrosslinked rubber, were deassembled by dissolution in chloroform. This suggests that some of the tiny particles on the road were not resuspended because of their adsorption on the APWP surface. For the TRWPs, the initial shapes were retained after the chloroform treatment as shown in Fig. 7, but many mineral particles on the surface are detached. The separation of many mineral particles from the TRWP is due to the swelling of the TWP and the penetration of chloroform between the mineral particles and the TWP surface.

The amounts of the chloroform-dissolved components in the HDWP samples are summarized in Table 5. The ratios of the chloroform-dissolved components in the winter HDWP samples ($11.3\text{--}28.9 \text{ wt}\%$) were the highest, while those in the summer HDWP samples ($0.3\text{--}1.4 \text{ wt}\%$) were the lowest. These results imply that the binder components are more abraded from the road pavement by traffic during the cold season, but they are less detached from the road pavement in the hot season. This is because the binder components become increasingly stiff at cold temperatures, resulting in breakage of the binder region in the asphalt pavement by traffic. Under hot and warm weather conditions, the binder components would be flexible and could not be broken.

The variations in the ratios of the chloroform-dissolved components in the HDWP samples collected in the winter and spring seasons showed specific trends depending on the particle size, i.e., the ratios decreased as the particle size increased. This indicates that the APWPs generated during winter and spring contain more binder components as the particle size decreases. The variations in the ratios of the chloroform-dissolved components in the HDWP samples collected during the summer and fall seasons did not show a specific trend. However, the two variations were reverse: for the summer HDWP sample, the ratio in the sample of size $212\text{--}500 \mu\text{m}$ was higher than those in the samples of size $106\text{--}212$ and $500\text{--}1000 \mu\text{m}$, although for the fall HDWP sample, the former was lower than the latter.

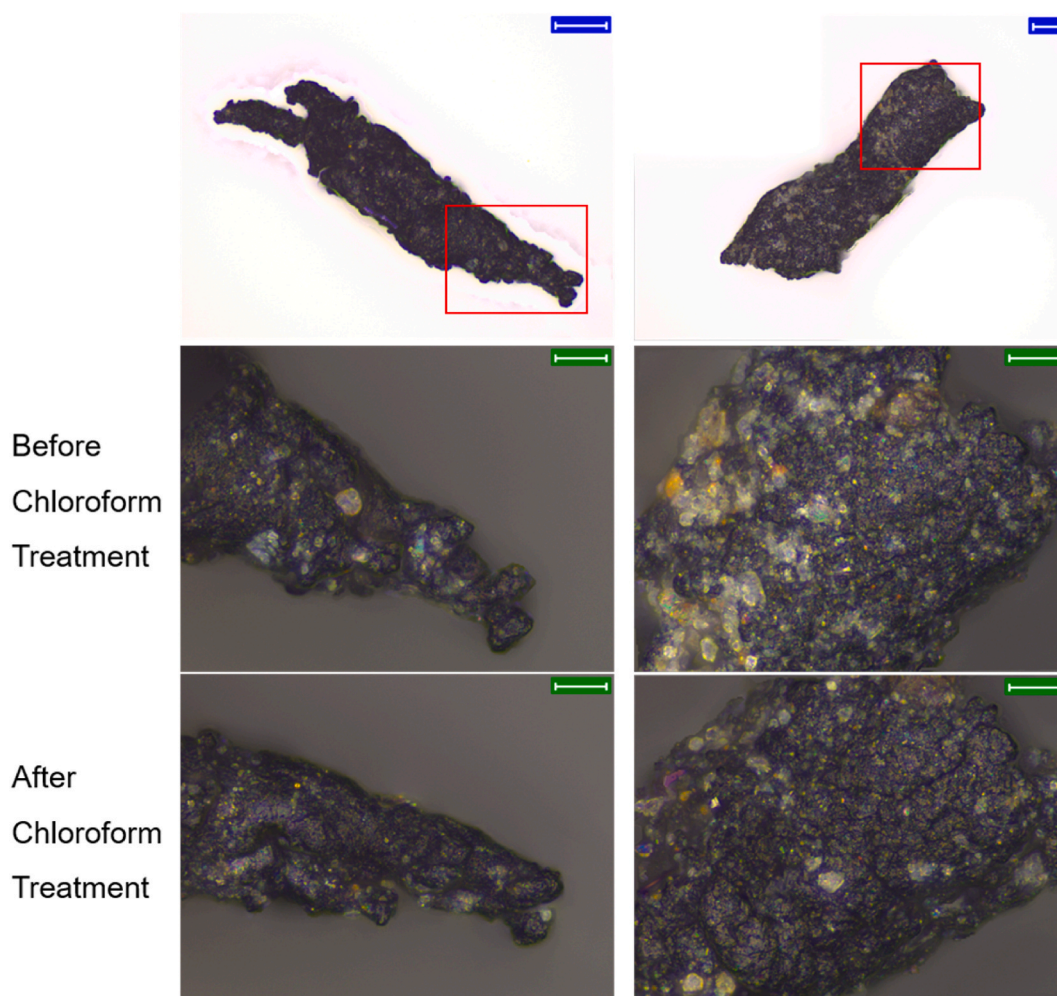


Fig. 7. Magnified images ($\times 200$ and 500) of the tire-road wear particle (TRWP) before and after the chloroform treatment. The blue and green scale bars are 50 and $20 \mu\text{m}$, respectively.

Table 5

Ratios of chloroform-dissolved components in the wear particles with high density ($>1.8 \text{ g cm}^{-3}$) (wt%).

Season	Wear particle size (μm)		
	106–212	212–500	500–1000
Winter	28.9	21.5	11.3
Spring	1.9	0.7	0.6
Summer	0.3	1.4	0.9
Fall	2.7	0.8	2.7

4. Conclusions

The particle size distributions of the road dust samples showed two opposite patterns: those of the samples collected in winter and spring decreased as the particle size decreased, whereas those of the samples collected in summer and fall tended to increase. Overall, the HDWPs in the road dust samples were higher than $80 \text{ wt}\%$; those in the winter road dust ($94.0\text{--}95.6 \text{ wt}\%$) were the highest, whereas those in the spring road dust ($82.7\text{--}9.7 \text{ wt}\%$) were the lowest. The average HDWP contents in road dust of $106\text{--}1000 \mu\text{m}$ were $95.1 \text{ wt}\%$, $85.3 \text{ wt}\%$, $90.4 \text{ wt}\%$, and $89.1 \text{ wt}\%$ for the winter, spring, summer, and fall seasons, respectively. The HDWP samples contained eight particle types, and the order of particle type distribution in the samples of size $106\text{--}1000 \mu\text{m}$ was $\text{MP} > \text{APWP} > \text{GP} > \text{GB} > \text{RPWP} > \text{PRP} > \text{PP} > \text{TRWP}$. Wear microparticles sourced from road abrasion can reach up to $95 \text{ wt}\%$. TRWPs were rarely detected in the samples of size $212\text{--}1000 \mu\text{m}$, and were detected in small amounts in the samples of size $106\text{--}212 \mu\text{m}$. The Zn content was much higher in small-sized samples than in large-sized samples. The Fe content was higher in winter than in other seasons.

Following chloroform treatment, the APWPs were divided into many particles, whereas the TRWPs retained their initial shapes; however, many mineral particles on the TWP surface were detached. The ratios of the chloroform-dissolved components in the winter HDWP samples (11.3–28.9 wt%) were the highest, while those in the summer HDWP samples (0.3–1.4 wt%) were the lowest, due to the seasonal differences in the stiffness of the binder components. HDWPs can be accumulated as sediments in rivers and seas, and some potentially harmful chemicals in HDWPs may be released into these aquatic ecosystems. Hence, suctioning of road dust is a better way to remove it than washing with water to avoid the sedimentation of road dust in aquatic systems. In the future, research on sedimentation rate of road dust in water depending on not only the type, size, and density of road dust but also water flow, velocity, and depth is necessary. For the particles smaller than 100 μm , the organic components such as TWPs and PPs in the sample can be analyzed using pyrolysis-gas chromatography/mass spectrometry (Py-GC/MS), while the inorganic components can be analyzed using XRF or inductively coupled plasma-mass spectrometry (ICP-MS). However, it may be not possible to correctly determine their sources such as MP, GB, GP, and APWP without classification with the naked eye.

CRedit authorship contribution statement

Uiyeong Jung: Writing – original draft, Visualization, Validation, Investigation, Formal analysis, Data curation. **Sung-Seen Choi:** Writing – review & editing, Writing – original draft, Supervision, Resources, Project administration, Methodology, Funding acquisition, Conceptualization.

Data and code availability statement

Data will be made available on request.

Funding

This work was supported by the Technology Innovation Program funded by the Ministry of Trade, Industry and Energy, Republic of Korea (Project Number 20010851).

Declaration of competing interest

The authors declare that they have no known competing financial interests or personal relationships that could have appeared to influence the work reported in this paper.

References

- [1] X. Chang, R. Zhang, Y. Xiao, X. Chen, X. Zhang, G. Liu, Mapping of publications on asphalt pavement and bitumen materials: a bibliometric review, *Constr. Build. Mater.* 234 (2020) 117370.
- [2] L.P. Thives, E. Ghisi, Asphalt mixtures emission and energy consumption: a review, *Renew. Sustain. Energy Rev.* 72 (2017) 473–484.
- [3] T. Wang, F. Xiao, X. Zhu, B. Huang, J. Wang, S. Amirkhanian, Energy consumption and environmental impact of rubberized asphalt pavement, *J. Clean. Prod.* 180 (2018) 139–158.
- [4] S. Abo-Qudais, H. Al-Shweily, Effect of aggregate properties on asphalt mixtures stripping and creep behavior, *Constr. Build. Mater.* 21 (2007) 1886–1898.
- [5] A. Behnood, M.M. Gharehveran, Morphology, rheology, and physical properties of polymer-modified asphalt binders, *Eur. Polym. J.* 112 (2019) 766–791.
- [6] S. Cui, B.R.K. Blackman, A.J. Kinloch, A.C. Taylor, Durability of asphalt mixtures: effect of aggregate type and adhesion promoters, *Int. J. Adhes. Adhes.* 54 (2014) 100–111.
- [7] F. Dong, W. Zhao, Y. Zhang, J. Wei, W. Fan, Y. Yu, Z. Wang, Influence of SBS and asphalt on SBS dispersion and the performance of modified asphalt, *Constr. Build. Mater.* 62 (2014) 1–7.
- [8] T. Schnell, H.T. Zwahlen, Driver preview distances at night based on driver eye scanning recordings as a function of pavement marking retroreflectivities, *Transp. Res. Rec.* 1692 (1999) 129–141.
- [9] K.M. Wenzel, T.E. Burghardt, A. Pashkevich, W.A. Buckermann, Glass beads for road markings: surface damage and retroreflection decay study, *Appl. Sci.* 12 (2022) 2258.
- [10] I. Järslskog, A.-M. Strömvall, K. Magnusson, M. Gustafsson, M. Polukarova, H. Galfi, M. Aronsson, Y.A. Skold, Occurrence of tire and bitumen wear microplastics on urban streets and in sweepsand and washwater, *Sci. Total Environ.* 729 (2020) 138950.
- [11] U.Y. Jung, S.-S. Choi, A variety of particles including tire wear particles produced on the road, *Elast. Compos.* 56 (2021) 85–91.
- [12] U.Y. Jung, S.-S. Choi, Classification and characterization of tire-road wear particles in road dust by density, *Polymers* 14 (2022) 1005.
- [13] U.Y. Jung, S.-S. Choi, Characteristics in densities and shapes of various particles produced by friction between tire tread and road surface, *Elast. Compos.* 57 (2022) 92–99.
- [14] M.L. Kreider, J.M. Panko, B.L. McAtee, L.I. Sweet, B.L. Finley, Physical and chemical characterization of tire-related particles: comparison of particles generated using different methodologies, *Sci. Total Environ.* 408 (2010) 652–659.
- [15] I. Järslskog, D. Jaramillo-Vogel, J. Rausch, S. Perseguers, M. Gustafsson, A.-M. Strömvall, Y. Andersson-Sköld, Differentiating and quantifying carbonaceous (tire, bitumen, and road marking wear) and non-carbonaceous (metals, minerals, and glass beads) non-exhaust particles in road dust samples from a traffic environment, *Water Air Soil Pollut.* 233 (2022) 375.
- [16] E. Apeayei, M.S. Bank, J.D. Spengler, Distribution of heavy metals in road dust along an urban-rural gradient in Massachusetts, *Atmos. Environ.* 45 (2011) 2310–2323.
- [17] P.J. Kole, A.J. Lohr, F.G.A.-J. van Bellegem, A.M.J. Ragea, Wear and tear of tyres: a stealthy source of microplastics in the environment, *Int. J. Environ. Res. Public Health* 14 (2017) 1265.
- [18] F. Sommer, V. Dietze, A. Baum, J. Sauer, S. Gilge, C. Maschowski, R. Gieré, Tire abrasion as a major source of microplastics in the environment, *Aerosol Air Qual. Res.* 18 (2018) 2014–2028.
- [19] W.E. Dietrich, Settling velocity of natural particles, *Water Res. Res.* 18 (1982) 1615–1626.
- [20] L. Gelhardt, U. Dittmer, A. Welker, Relationship of particle density and organic content in sieve fractions of road-deposited sediments from varying traffic sites based on a novel data set, *Sci. Total Environ.* 794 (2021) 148812.

- [21] H.M. Haynes, K.G. Taylor, J. Rothwell, P. Byrne, Characterisation of road-dust sediment in urban systems: a review of a global challenge, *J. Soils Sediments* 20 (2020) 4194–4217.
- [22] S.H. Rommel, L. Gelhardt, A. Welker, B. Helmreich, Settling of road-Deposited sediment: influence of particle density, shape, low temperatures, and deicing salt, *Water* 12 (2020) 3126.
- [23] F. Alsaadi, P.V. Hodson, V.S. Langlois, An embryonic field of study: the aquatic fate and toxicity of diluted bitumen, *Bull. Environ. Contam. Toxicol.* 100 (2018) 8–13.
- [24] E.J.M. Blokker, B.M. van de Ven, C.M. de Jongh, P.G.G. Slaats, Health implications of PAH release from coated cast iron drinking water distribution systems in The Netherlands, *Environ. Health Perspec.* 121 (2013) 600–606.
- [25] H.C.A. Brandt, P.C. de Groot, Aqueous leaching of polycyclic aromatic hydrocarbons from bitumen and asphalt, *Water Res.* 35 (2001) 4200–4207.
- [26] P. Klöckner, B. Seiwert, S. Weyrauch, B.I. Escher, T. Reemtsma, S. Wagner, Comprehensive characterization of tire and road wear particles in highway tunnel road dust by use of size and density fractionation, *Chemosphere* 279 (2021) 130530.
- [27] Z.-M. Li, V.K. Pal, P. Kannan, W. Li, K. Kannan, 1,3-Diphenylguanidine, benzothiazole, benzotriazole, and their derivatives in soils collected from northeastern United States, *Sc. Total Environ.* 887 (2023) 164110.
- [28] Z. Tian, H. Zhao, K.T. Peter, M. Gonzalez, J. Wetzel, C. Wu, X. Hu, J. Prat, E. Mudrock, R. Hettinger, A.E. Cortina, R.G. Biswas, F.V.C. Kock, R. Soong, A. Jenne, B. Du, F. Hou, H. He, R. Lundeen, A. Gilbreath, R. Sutton, N.L. Scholz, J.W. Davis, M.C. Dodd, A. Simpson, J.K. McIntyre, E.P. Kolodziej, A ubiquitous tire rubber-derived chemical induces acute mortality in coho salmon, *Science* 371 (2021) 185–189.
- [29] T. Grosgees, Retro-reflection of glass beads for traffic road stripe paints, *Opt. Mater.* 30 (2008) 1549–1554.
- [30] J. Seo, W. Kim, S. Bae, J. Kim, Influence of loading procedure of liquid butadiene rubber on properties of silica-filled tire tread compounds, *Elast. Compos.* 57 (2022) 129–137.
- [31] S. Song, J. Jeong, J.U. Ha, D. Park, G. Ryu, D. Kim, K. Hwang, S. Chung, W. Kim, Influence of blending method on the generation of wear particulate matters and physical properties in TBR tire tread compounds, *Elast. Compos.* 58 (2023) 161–172.
- [32] Y.M. Yun, J.H. Lee, M.C. Choi, J.W. Kim, H.M. Kang, J.W. Bae, A study on the effect of petroleum resin on vibration damping characteristics of natural rubber composites, *Elast. Compos.* 56 (2021) 201–208.
- [33] M.A. Fayad, M.T. Chaichan, H.A. Dhahad, A.A. Al-Amiery, W.N.R.W. Isahak, Reducing the effect of high sulfur content in diesel fuel on NO_x emissions and PM characteristics using a PPCI mode engine and gasoline-diesel blends, *ACS Omega* 7 (2022) 37328–37339.
- [34] V. Rezvani, H. Saghi, Characteristics and preparation method of sulfur extended asphalt mixtures, *Am. J. Civil Eng.* 3 (2015) 69–74.
- [35] T. Grigoratos, G. Martini, Brake wear particle emissions: a review, *Environ. Sci. Pollut. Res.* 22 (2015) 2491–2504.
- [36] E. Chae, U. Jung, S.-S. Choi, Types and concentrations of tire wear particles (TWPs) in road dust generated in slow lanes, *Environ. Pollut.* 346 (2024) 123670.
- [37] E. Chae, S.-S. Choi, Quantification of road dust transfer to central lane bus stop from other lanes using tire tread rubber markers of bus and passenger vehicle through pyrolytic technique, *J. Anal. Appl. Pyrolysis* 179 (2024) 106493.
- [38] Y. Ren, W. Li, Q. Jia, Y. Zhao, C. Qu, L. Liu, J. Liu, C. Wu, Separation and quantification of tire and road wear particles in road dust samples: bonded-sulfur as a novel marker, *J. Hazard Mater.* 465 (2024) 133089.
- [39] H. Li, C. Cui, A.A. Temitope, Z. Feng, G. Zhao, P. Guo, Effect of SBS and crumb rubber on asphalt modification: a review of the properties and practical application, *J. Traffic Transp. Eng. (Engl. Ed.)* 9 (2022) 836–863.